MAVFlow: Preserving Paralinguistic Elements with Conditional Flow Matching for Zero-Shot AV2AV Multilingual Translation

Sungwoo Cho[1] Jeongsoo Choi[2] Sungnyun Kim[1] Se-Young Yun[1]
[1]KAIST AI [2]KAIST EE
{peter8526, jeongsoo.choi, ksn4397, yunseyoung}@kaist.ac.kr

Abstract

Despite recent advances in text-to-speech (TTS) models, audio-visual-to-audio-visual (AV2AV) translation still faces a critical challenge: maintaining speaker consistency between the original and translated vocal and facial features. To address this issue, we propose a conditional flow matching (CFM) zero-shot audio-visual renderer that utilizes strong dual guidance from both audio and visual modalities. By leveraging multimodal guidance with CFM, our model robustly preserves speaker-specific characteristics and enhances zero-shot AV2AV translation abilities. For the audio modality, we enhance the CFM process by integrating robust speaker embeddings with x-vectors, which serve to bolster speaker consistency. Additionally, we convey emotional nuances to the face rendering module. The guidance provided by both audio and visual cues remains independent of semantic or linguistic content, allowing our renderer to effectively handle zero-shot translation tasks for monolingual speakers in different languages. We empirically demonstrate that the inclusion of high-quality mel-spectrograms conditioned on facial information not only enhances the quality of the synthesized speech but also positively influences facial generation, leading to overall performance improvements in LSE and FID score. Our code is available at https://github.com/Peter-SungwooCho/MAVFlow.

1. Introduction

With the rapid proliferation of multimedia content and increasing cross-cultural interactions, the expansion from one language to another has become essential to enrich user engagement and comprehension. Traditional approaches in language translation, such as subtitle processing via neural machine translation (NMT) [42] or single-modality methods like speech-to-speech translation and dubbing [20], often fail to deliver a fully immersive experience. For instance, in dubbed films, discrepancies between the original visual content and the dubbed audio can lead to unnatural lip synchronization and a mismatch between the expected and dubbed voices. Such inconsistencies disrupt the viewer's concentration and diminish the overall experience. The adverse effects of audio-visual incongruence on user perception have been substantiated by the McGurk effect [43]; notably, when the dubbed voice deviates from the expected voice of original actors, the naturalness of the content significantly deteriorates [32].

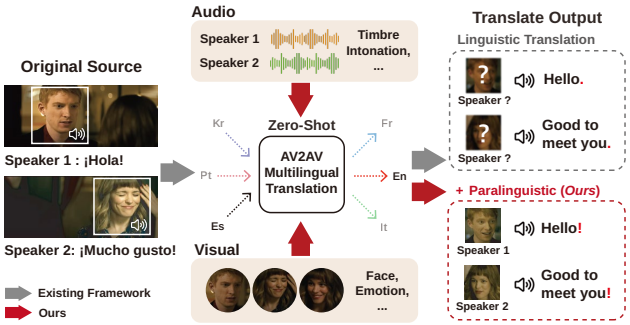

Figure 1. Overview of the existing audio-visual translation (AV2AV) framework. Conventional AV2AV methods primarily focus on linguistic content, often neglecting crucial paralinguistic features, such as speaker identity and emotional nuance, which are essential for maintaining consistent speaker characteristics.

At a fundamental level, the transition from single-modality to dual-modality translation is achievable via cascaded approaches. A typical pipeline involves using an automatic speech recognition (ASR) model [3, 52] to transcribe the source audio into text, subsequently applying NMT [15, 19] for language conversion, and finally synthesizing speech via text-to-speech (TTS) systems [7, 8, 65] in conjunction with talking face generation (TFG) models [49, 51, 69]. However, such cascaded methods are complex and often suffer from significant information loss due to repeated modality transformations and intermediate text representations. To overcome these challenges, direct audio-visual-to-audio-visual (AV2AV) translation approaches have been introduced [12, 13, 25]. These methods bypass textual representations by leveraging discrete units obtained from self-supervised multimodal models (*e.g.*,

multilingual AV-HuBERT [13, 55]), enabling a more direct and efficient translation of audio-visual source inputs.

Despite these advances, the AV2AV translation still faces a critical challenge: preserving speaker consistency (*e.g.*, tone, pitch, or facial expressions) between the original and translated audio-visual data (as shown in Figure 1). This limitation is exacerbated by the absence of datasets wherein the same speaker articulates identical content in multiple languages, necessitating zero-shot strategies for speaker preservation. Current AV2AV approaches [12, 13] adopt a simple architecture that relies on using speaker embeddings, combining speaker-specific d-vectors [62] within the speech vocoder [30, 51]. This yet underexplored structure of AV2AV, which does not employ advanced conditional generation techniques, still restricts its ability to maintain speaker consistency. Moreover, generating audio and visual components are separated, using a single-modality embedding in each part. This has limitations from a multimodal perspective since only the reference audio is used, while visual cues could also be considered for speech generation.

In this study, to *preserve paralinguistic elements* of speakers during the *linguistic translation*, we propose MAVFlow, a Conditional Flow Matching (CFM) [44] based zero-shot audio-visual renderer that leverages dual guidance from audio and visual modalities. Notably, for ideal multilingual translation scenarios, a speaker's voice characteristics and facial information (*e.g.*, appearance or emotion) must remain consistent regardless of language [1, 5, 67]. Based on this hypothesis, we adopt a guidance strategy that utilizes speaker embeddings from audio and emotion embeddings from visual input. This strategy enables the complementary capture of paralinguistic information, which are commonly shared across both audio and visual modalities.

Furthermore, MAVFlow leverages the Optimal Transport (OT) CFM's structural advantages in integrating a multimodal guidance. OT-CFM [44] facilitates learning a conditional speech distribution, enhancing zero-shot performances and guidance-based control, making it an ideal approach for preserving paralinguistics in AV2AV translation. MAVFlow incorporates x-vector-based speaker embeddings [56] of audio and facial emotion embeddings [60] of visual inputs, directly guiding the flow matching generative module. Additionally, OT-CFM significantly improves speech synthesis performance and enables more efficient sampling with fewer steps. Thus, MAVFlow achieves enhanced speaker consistency while producing seamless audio-visual translation results in cross-lingual scenarios. Our contributions are summarized as follows:

- We propose MAVFlow, integrating discrete speech units with OT-CFM to efficiently synthesize high-quality mel-spectrograms for advanced audio-visual translation.
- We transmit paralinguistic speaker characteristics from both audio and visual modalities within the latent space of the OT-CFM model, thereby achieving robust zero-shot capabilities in cross-lingual scenarios.
- We empirically demonstrate that our dual guidance improves the consistency of speaker identity in synthesized speech by an average of 36% on the MuAViC dataset [3], while enhancing face generation with gains in lip-sync accuracy ($+0.87$) and visual quality score (-0.61) on textless system.
- We also confirm that MAVFlow effectively represents emotion in both audio and visual generation on the CREMA-D dataset [6].

2. Related Works

2.1. Spoken Language Translation

Spoken Language Translation (SLT) aims to convert spoken language in one language into another language, promoting natural cross-lingual interaction. Traditional SLT typically adopt cascaded approaches [41, 47] for speech-to-speech translation (S2ST), chaining ASR, NMT, and TTS. Although widely used, cascaded methods suffer from cumulative errors, latency, and loss of speaker-specific prosodic and paralinguistic features [27, 66]. To reduce these issues, research has shifted toward end-to-end SLT methods that translate speech directly [28, 46], and even textless approaches that eliminate the reliance on textual representations [29, 35].

Despite advances, S2ST systems primarily focus on audio signals, often neglecting the alignment between translated speech and visual information, which is crucial for cross-lingual scenarios such as video conferencing or dubbing. This can lead to lip-sync mismatches [32, 43], disrupting realistic multimodal experiences. Speech-driven TFG has been explored to synchronize video with translated speech [33, 64]. More recently, TransFace [12] and AV2AV [13] jointly generate synchronized audio and visual outputs. However, achieving natural cross-lingual experiences remains challenging, particularly in preserving speaker identity and maintaining emotional consistency.

2.2. Flow Matching for Generative Modeling

Generative models based on diffusion process [23, 58] have demonstrated remarkable performance across various domains, including image [16, 53], speech [26, 50], audio [10, 31], and video [4, 24], by iteratively denoising to generate high-fidelity outputs. Despite their impressive quality, diffusion-based models often require numerous sampling steps, limiting their practicality for real-time or large-scale applications. Flow matching [36, 37] models address this limitation by learning direct stochastic paths between distributions, enabling efficient and high-quality generation in fewer steps [38]. This approach has been successfully applied to various tasks [18, 34, 39, 44].

Recent works have explored conditioning flow matching models to enable following conditions while maintaining high-quality generation, becoming prominent in generative modeling. Additionally, conditioning with multiple inputs has emerged as a promising direction [45], and conditional flow matching model successfully leverage these conditions to produce aligned and controllable outputs [21, 63]. However, effectively extracting and utilizing relevant information from multimodal signals for conditioning remains in its early stages.

3. Preliminaries

3.1. Audio-Visual Speech Unit Translation

Recent advances in direct audio-visual-to-audio-visual translation have leveraged discrete speech units to bypass intermediate text transcription, thereby avoiding delays and error propagation of cascaded systems and expanding applicability [12]. To obtain translated AV units, our system follows two-stage procedure. First, we extract discrete AV units from an input sequence using the unit extractor, m-AVHuBERT [13], which has been pretrained on 7,000 hours of multilingual audio-visual data. Second, we pass the extracted discrete units to a unit-to-unit (U2U) translation module [13], which translates them into the counterparts of target language. The translated units are subsequently converted into intermediate features (mel-spectrograms) via CFM, and finally transformed back into audio-visual form through the vocoder and face decoder. Notably, both the unit extractor and the U2U translation module are identical to those used in our prior work [13], thus ensuring consistency in performance.

3.2. Optimal Transport CFM

Conditional Flow Matching (CFM) is a framework that leverages conditional flows to train generative models, particularly applied to generate mel-spectrograms in audio synthesis tasks [17, 44]. Unlike conventional flow-based models, which learn a bijective mapping between a simple prior distribution (*e.g.*, Gaussian noise) and a mel-spectrogram target distribution, CFM directly optimizes the trajectory connecting the two distributions using optimal transport (OT). This facilitates the effective generation of data distributions conditioned on auxiliary information, such as text embedding, audio-visual features, or speaker embeddings, by learning an appropriate conditional vector field [36, 61].

In our framework, data distribution $p(X)$ is connected to a mel-spectrogram representations, which are connected to a noise distribution $\pi(X)$ through a continuous trajectory $\{X_t\}_{t=0}^{1}$. Here, $p(X)$ and $\pi(X)$ denote the mel-spectrogram data distribution (target distribution) and the noise prior distribution, respectively. The trajectory that continuously transforms $\pi(X)$ into $p(X)$, which is optimized by OT-CFM in the sense of optimal transport. Specifically, for $t \in [0, 1]$,

$$\frac{d}{dt}\phi_t(X) = \nu_t^\star(\phi_t(X), t) \tag{1}$$

where $\nu_t^\star$ is the optimal vector field that solves the OT problem. During training, we estimate $\nu_t(\phi_t(X), t)$ to approximate $\nu_t^\star$. In our approach, the condition $\mathbf{c}$ corresponds to audio-visual units with various guidance. Consequently, the evolution of the data is modeled as

$$\frac{d}{dt}\phi_t(X) = \nu_t(\phi_t(X), t \mid \mathbf{c}) \tag{2}$$

and we train a conditional vector field ν_t that integrates both audio and visual features. The OT-CFM optimization objective function is defined by

$$\min_\theta \mathbb{E}_{t,\phi_t(X)|\mathbf{c}}\left[\|\nu_t(\phi_t(X), t \mid \mathbf{c}) - \nu_t^\star(\phi_t(X), t)\|^2\right] \tag{3}$$

where $\nu^\star$ is approximated during training via score matching or stochastic path sampling techniques.

4. MAVFlow

To effectively preserve speaker-specific characteristics such as voice consistency and facial expressions in multilingual audio-visual translation, we introduce MAVFlow, comprising four main stages: *(i) Audio-Visual Speech Unit Translation*, which we have outlined in Section 3.1; *(ii) Duration Length Regulator*; *(iii) Multimodal Guidance*; and *(iv) CFM-based Zero-Shot AV-Renderer* which effectively integrates paralinguistic multimodal guidance with linguistic audio-visual units to synthesize audio-visual outputs. The overall architecture and pipeline of MAVFlow are illustrated in Figure 2.

4.1. Duration Length Regulator

Since the output of the U2U translation module is deduplicated, it is necessary to predict and expand the duration of each unit. To achieve this, we employ a *Duration Length Regulator*, adapting duration prediction concepts previously explored in TTS synthesis specifically for our audio-visual translation task. We adopt a similar duration prediction structure and loss function from AV2AV [13], using two 1D-convolution layers with a classifier, where the objective function is the MSE loss in the log domain. However, our *Duration Length Regulator* differs in that it interpolates the generated audio to match the length of the original source audio. This design addresses a critical constraint in real-world movie dubbing scenarios, where the video length must remain consistent before and after translation—an aspect not considered in AV2AV.

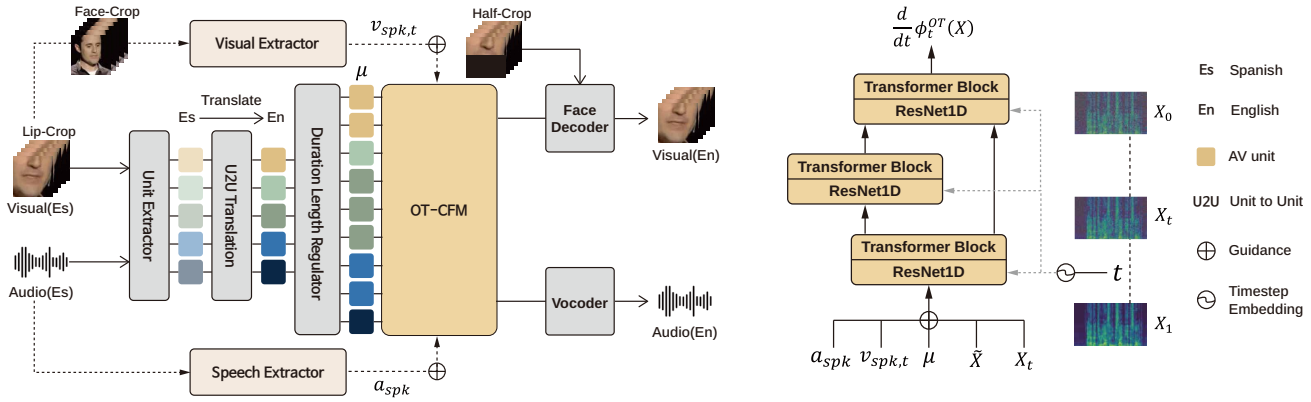

(a) Overall framework of MAVFlow

(b) OT-CFM decoder structure

Figure 2. Overall framework and detailed architecture of MAVFlow. (a) An overview of the proposed MAVFlow translation system. (b) OT-CFM's Transformer decoder structure with multimodal guidance $\mathbf{a}_{\text{spk}}$ and $\mathbf{v}_{\text{spk,t}}$ to generate guided mel-spectrogram.

4.2. Multimodal Guidance

In the process of generating mel-spectrograms based on the linguistic information of the AV speech unit, conventional methods [13] relying solely on audio often fall short in accurately capturing visual aspects such as the speaker's emotional state or facial expressions. Particularly in multilingual audio-visual translation, preserving the speaker's natural characteristics requires incorporating not only vocal attributes but also paralinguistic elements like facial expressions. To address this limitation, our approach introduces multimodal guidance by integrating both *speaker voice embeddings* extracted from audio and *speaker facial emotion embeddings* derived from visual inputs. This dual guidance strategy enables a clearer transmission of speaker-specific traits across both modalities, resulting in more consistent and natural synthesis of voice and emotional expression in multilingual translation scenarios.

Speaker voice embedding. To capture paralinguistic elements from the audio modality, we use a pretrained speaker encoder to extract x-vectors [56], which encode the speaker's unique timbre and speaking style. These robust speaker embeddings are particularly suitable for our cross-lingual scenario. Specifically, in training phase we calculate x-vectors for multiple utterances from the same speaker, then average them to form a *speaker-level* embedding $\mathbf{a}_{\text{spk}}$:

$$\mathbf{a}_{\text{spk}} = \frac{1}{N}\sum_{i=1}^{N}\mathbf{a}_{\text{utt},i} \tag{4}$$

where $\mathbf{a}_{\text{utt},i}$ is the x-vector extracted from the i-th utterance of a given speaker, and N is the total number of utterances for that speaker. The use of such an averaged speaker embedding allows the model to learn general speaker information during training, thereby enabling the model to robustly learn common speaker traits.

To guide mel-spectrogram generation using a global speaker representation, we concatenate this speaker embedding with the latent feature of each frame. This frame-level concatenation ensures that synthesized speech consistently reflects the speaker's unique characteristics. During inference, we directly utilize utterance-specific embedding $\mathbf{a}_{\text{utt},i}$, capturing and preserving fine-grained variations unique to each utterance. By employing distinct speaker embeddings for each phase, our model learns general, global paralinguistic information during training, while effectively capturing local, utterance-specific paralinguistic variations during inference, ultimately enhancing the quality of the generated mel-spectrograms.

Speaker facial emotion embedding. In addition to audio cues, we incorporate paralinguistic speaker face emotional embeddings to ensure that the model also learns from visual characteristics of the speaker. We adopt EmoFAN [60] to extract facial emotion embeddings from each frame. Specifically, emotional information in a speaker's utterance can vary dynamically across frames. For instance, a speaker may start smiling partway through an utterance or shift emotional states over time. Thus, distinct emotion embeddings $\mathbf{v}_{\text{spk},t}$ are added as guidance for generating each mel-spectrogram frame X_t:

$$\mathbf{v}_{\text{spk},t} = \text{Emo}(\mathbf{f}_{\text{t}}) \tag{5}$$

where $\mathbf{v}_{\text{spk},t}$ denotes the face embedding of the t-th sampled frame $\mathbf{f}_t$, and $\text{Emo}(\cdot)$ is facial emotion extractor. This reflects a distinctive aspect of the cross-lingual scenario, where frame-level speaker audio characteristics vary according to language-specific phonetic and prosodic differences (*e.g.*, variations in accent, intonation patterns, rhythm, and stress placement), whereas emotional information remains consistent across languages.

4.3. CFM-based Zero-Shot AV-Renderer

The CFM-based AV-Renderer integrates translated AV units containing linguistic information with multimodal guidance carrying paralinguistic features. The AV units utilize interpolation to effectively synchronize audio and visual modalities temporally. Additionally, speaker embeddings, as global paralinguistic features, are uniformly added to every frame to maintain consistent emotional and speaker characteristics, while visual embeddings are applied individually across temporal frames. This ensures both temporal and linguistic coherence, resulting in a mel-spectrogram that naturally blends the speaker's facial expressions with their acoustic properties.

Guided mel generation. To effectively synthesize intermediate mel-spectrograms from audio-visual units, MAVFlow incorporates multimodal information to capture paralinguistic features, as introduced in Section 4.2. Specifically, we employ CFM to guide the mel-spectrogram generation process, optimizing an objective defined as:

$$\mathcal{L}_{OT-CFM} = \mathbb{E}_{t,p_0(X_0),q(X_1)}\Big[\omega_t\big(\phi_t^{OT}(X_0,X_1) \mid X_1\big) - \nu_t\big(\phi_t^{OT}(X_0,X_1) \mid \theta\big)\Big]. \tag{6}$$

where $\phi_t^{OT}(X_0,X_1)$ is $(1-(1-\sigma)t)X_0 + tX_1$ and $\omega_t\left(\phi_t^{OT}(X_0,X_1)\middle|X_1\right)$ is $X_1-(1-\sigma)X_0$.

The multimodal embeddings consist of a global speaker embedding $\mathbf{a}_{\text{spk}}$, uniformly applied across all frames, and a frame-level emotion embedding $\mathbf{v}_{\text{spk,t}}$, dynamically varying per timestep. These embeddings, together with the linguistic speech tokens $\{\mu_l\}_{1:L}$ and the masked mel-spectrogram $\tilde{X}_1$, are jointly fed into the neural network N_θ to match the conditional vector field parameterized by θ, facilitating the integration of global speaker characteristics and local emotional dynamics (as shown in Figure 2a).

$$\begin{aligned}&\nu_t\big(\phi_t^{OT}(X_0,X_1) \mid \theta\big)\\ &= N_\theta\big(\phi_t^{OT}(X_0,X_1), t; \mathbf{a}_{\text{spk}}, \mathbf{v}_{\text{spk,t}}, \{\mu_l\}_{1:L}, \tilde{X}_1\big)\end{aligned} \tag{7}$$

This strategic utilization of multimodal embeddings, which integrates complementary global speaker identity from audio and frame-level emotional dynamics from visual inputs, plays a crucial role in improving naturalness and speaker consistency in multilingual audio-visual translation.

5. Experiments

5.1. Implementation Details

Dataset. For training and evaluation, we utilize MuAViC [3], a multilingual audio-visual corpus comprising 1,200 hours of transcribed speech from thousands of speakers, curated from LRS3 [2] and mTEDx [54]. We use five languages: English, Spanish, French, Italian, and Portuguese. Since MuAViC does not contain emotion labels, we employ an additional dataset, CREMA-D [6], for emotion evaluation. CREMA-D consists of 7,442 short video clips featuring 91 adult actors expressing six different emotions: anger, disgust, fear, happy, neutral, and sad. Each clip captures an actor uttering a sentence while simultaneously providing facial expressions and vocal information, making it a suitable dataset for evaluating our model's performance on emotional maintenance.

Model description. MAVFlow uses the CFM model pretrained on the LibriTTS [68] as the initial point for more efficient learning. The model is trained on 8 RTX A6000 GPUs with a constant learning rate of 0.0001. The speaker embedding and emotional embedding extracted from each audio and visual input—originally 192 and 256 dimensions, respectively—are compressed to an 80-dimensional representation and used as guidance for the OT-CFM. To convert the generated mel-spectrogram into a raw audio waveform, we train HiFi-GAN [30] on the LRS3 dataset. We use the same multi-scale L1 and discriminator loss functions proposed in HiFi-GAN. For precise lip-sync and facial expression generation, we use pretrained Wav2Lip [51] on the LRS2 [57] dataset. Details about the inference time are provided in Appendix C.

5.2. Baseline Methods

There exist only two textless systems, AV2AV [13] and Transface [12], that directly utilize units without generating text in the intermediate process. However, our goal is to develop a zero-shot model that generates translated speech while maximally preserving the original speaker's paralinguistics. Therefore, Transface, which follows a similar approach to AV2AV but does not incorporate additional speaker embeddings—thus not supporting zero-shot audio generation—was excluded from our comparison. Accordingly, for reasonable performance comparison, we establish baselines by combining existing systems in a cascaded manner and compare our proposed method against them. Specifically, the cascaded systems are built based on the latest off-the-shelf pre-trained models such as AVSR [3], ASR [3], AV2T [3], A2T [3], NMT [8], TTS [7, 8], and TFG [51].

5.3. Evaluation

Audio evaluation. We assess our model by using speaker similarity metrics. SS (speaker similarity) leverages ERes2Net [11], providing a robust measure of how closely the synthesized speech matches the target speaker's identity. ERes2Net is a widely used model trained on the VoxCeleb2 [14] dataset for speaker classification. Since SS alone is insufficient to evaluate the temporal alignment between generated and target mel-spectrograms, we addi-

Table 1. Comparison of zero-shot speaker similarity scores between X-En translated speech and native speech for traditional cascaded systems and direct textless systems. En: English, Es: Spanish, Fr: French, It: Italian, Pt: Portuguese.

	Method	SS ↑	DTW ↓	DTW-SL ↓
(a) Es-En	GT (Es audio)	1.0	0.0	0.0
	4-Stage Cascaded System[a]	0.42	11.41	17.07
	3-Stage Cascaded System[b]	0.42	11.46	16.74
	2-Stage Cascaded System[c]	0.07	11.23	14.18
	Direct System (AV2AV)	0.35	9.96	12.94
	MAVFlow (ours)	**0.49**	**9.60**	**12.47**
(b) Fr-En	GT (Fr audio)	1.0	0.0	0.0
	4-Stage Cascaded System	0.34	10.75	17.00
	3-Stage Cascaded System	0.35	10.90	16.97
	2-Stage Cascaded System	0.02	10.78	13.79
	Direct System (AV2AV)	0.31	9.92	12.46
	MAVFlow (ours)	**0.51**	**8.76**	**10.97**
(c) It-En	GT (It audio)	1.0	0.0	0.0
	4-Stage Cascaded System	0.41	11.91	17.27
	3-Stage Cascaded System	0.41	11.80	16.79
	2-Stage Cascaded System	0.05	11.23	13.70
	Direct System (AV2AV)	0.37	10.44	14.75
	MAVFlow (ours)	**0.53**	**9.36**	**11.43**
(d) Pt-En	GT (Pt audio)	1.0	0.0	0.0
	4-Stage Cascaded System	0.36	11.12	17.89
	3-Stage Cascaded System	0.35	10.97	17.65
	2-Stage Cascaded System	0.11	10.89	13.72
	Direct System (AV2AV)	0.30	9.82	12.38
	MAVFlow (ours)	**0.48**	**9.14**	**11.53**

[a] AVSR [3] + NMT [19] + TTS [8] + TFG [51]
[b] AV2T [3] + TTS [8] + TFG [51]
[c] A2A [29] + TFG [51]

tionally adopt Mel Cepstral Distortion with Dynamic Time Warping (MCD-DTW) [9] and its speech-length weighted variant (MCD-DTW-SL) [9]. The SL variant further accounts for speech duration, providing a more comprehensive quality metric. We then examine translation quality with the ASR-BLEU score. Specifically, an ASR system is used to transcribe the generated audio, and the resulting text is compared against the ground-truth transcription to calculate the BLEU score [48]. Additionally, to evaluate the accuracy of emotion recognition, we assess the audio generated by each system using the pretrained emotion2vec [40].

Visual evaluation. For visual quality assessment, we employ Lip Sync Error (LSE) confidence and distance (-C/-D) [51] and Fréchet Inception Distance (FID) [22], where the LSE metrics quantify the synchronization accuracy of lip movements relative to the audio, while FID measures the distributional similarity between generated frames and real images. Additionally, to measure emotional accuracy from the generated visual frames, we utilize a 6-class[1] pretrained MAE-DFER [59] model for emotion classification. Also, emotion embedding cosine similarity (ES) is used to complement class-wise accuracy, which may miss subtle emotional variations due to its fixed set of classes.

Human evaluation. We have conducted subjective evaluations to capture the human perception of generated audio quality. We perform a Mean Opinion Score (MOS) test that includes two factors: MOS-Similarity, to gauge how closely the synthesized speech resembles the target speaker's voice, and MOS-Naturalness, which evaluates fluency and overall realism. We have recruited 21 participants, each rating a total of 8 audio samples per method. Our evaluation set consists of four different methods: MAVFlow, a 4-stage cascaded system, a 3-stage cascaded system, and AV2AV. To maintain objectivity and avoid excessive evaluations by the assessors, the 2-stage cascaded system, which showed relatively poor performance in Table 1, was excluded. Additionally, since the ground truth audio is in the original language before translation, it was excluded to ensure fairness in the evaluation.

[1] Neutral, Happy, Sad, Angry, Disgust, and Fear

Table 2. Comparison of zero-shot speaker similarity scores of generated audio for traditional cascaded systems and direct systems, with additional emotion evaluation on the CREMA-D dataset.

Method	Emo-Acc (%) ↑	SS ↑	DTW ↓	DTW-SL ↓
GT	81.95	1.0	0.0	0.0
GT Mel + Vocoder	68.41	0.76	1.75	1.75
ASR + YourTTS [7]	17.52	0.40	9.02	11.78
ASR + XTTS [8]	28.55	**0.46**	11.98	17.68
Direct System (AV2AV)	33.66	0.33	7.84	7.88
MAVFlow (ours)	**36.46**	0.39	**7.30**	**7.36**

5.4. Zero-shot Audio Translation Result

Speaker voice similarity. In Table 1, we evaluate the speaker similarity between the original speech and the speech generated after translation by our model and baseline models. As a result, MAVFlow generates the translated audio that has the highest speaker similarity score with the original voice, compared to the cascaded system and the baseline direct system (AV2AV). This implies that our audio-visual guidance demonstrates outstanding performance in preserving the speaker's identity. In addition, MAVFlow demonstrates superior performance relative to the baseline on the MCD-DTW and MCD-DTW-SL metrics, confirming that the speaker's pronunciation and timbre are well maintained. In particular, since MCD-DTW-SL also reflects duration consistency, this indicates that our duration length regulator has been effective. These results were obtained using speech generated by translating four source languages—Spanish, French, Italian, and Portuguese—into English. In generating the final translated speech, the speaker embedding extracted from the non-translated original speech and the emotion embedding extracted from the face were used as guidance for the renderer.

Emotion evaluation. To evaluate how accurately the emotion in the speech generated after translation reflects the emotion of the original speech, we compare the proposed model with the baseline model (AV2AV) using the CREMA-D dataset. The evaluation is based on the emotional accuracy calculated by the emo2vec model, which

Table 3. Translation quality (ASR-BLEU score) for X-En translation comparison with cascaded system.

Method	Translation Modality	X-En Es-En	Fr-En	It-En	Pt-En
• *4-Stage*					
ASR + NMT + TTS + TFG	A→AV	28.66	30.55	23.54	26.14
AVSR + NMT + TTS + TFG	AV→AV	**28.70**	29.21	**24.54**	**26.30**
• *3-Stage*					
A2T + TTS + TFG	A→AV	24.06	27.01	21.92	24.11
AV2T + TTS + TFG	AV→AV	24.61	26.90	22.33	24.83
• *2-Stage (Textless)*					
A2A + TFG	A→AV	26.15	30.14	22.41	23.77
• *Direct (Textless)*					
AV2AV	AV→AV	26.57	31.27	23.24	24.51
MAVFlow (ours)	AV→AV	26.97	**31.33**	23.43	24.97

Table 4. Comparison of MOS scores between X-En translated speech and native speech for traditional cascaded systems and direct systems.

Method	Similarity ↑	Naturalness ↑
4-Stage Cascaded System	2.81	3.29
3-Stage Cascaded System	2.89	3.25
Direct System (AV2AV)	3.33	3.58
MAVFlow (ours)	**3.49**	**4.01**

examines how the target speech (the synthesized speech after translation) is classified into ground-truth emotion categories. In Table 2, the emotion2vec [40] model achieves approximately 82% classification accuracy on the ground-truth(GT) audio, serving as an upper bound for the emotion recognition model itself. In this experiment, our model achieves 36.5% emotional accuracy (+2.8%, +7.91%, and +18.94% compared to AV2AV, ASR + YourTTS [7], and ASR + XTTS [8] respectively), suggesting that it successfully synthesizes speech that preserves emotional traits.

Translation quality. In Table 3, we evaluate the translation quality using the ASR-BLEU score for different language pairs. The result demonstrates that MAVFlow achieves improved translation performance compared to AV2AV. Since we generated speech using the same unit translation model as AV2AV, this confirms that our model produces more accurate speech outputs when given identical units. These results suggest that our model leverages the structural advantages of CFM to enhance feature matching and rendering, thereby increasing both the accuracy and consistency of the generated speech. Furthermore, MAVFlow exhibits competitive translation quality when compared to the cascaded systems. This result implies that our dual modality guidance does not impair semantic quality during translation, which is also critical in AV2AV applications, while better preserving paralinguistic elements (as seen in Tables 1–2).

Table 5. Reconstruction visual quality performance on LRS3.

ID	Method	LSE-C ↑	LSE-D ↓	FID ↓
• *Ground Truth*				
C1	GT Audio-Visual	7.63	6.89	-
• *Cascaded System*				
C2	GT Audio + TFG	8.23	**6.75**	5.66
C3	GT Text + TTS + TFG	7.01	7.49	**5.38**
• *AV2AV*				
C4	GT AV Speech Unit	7.43	7.30	6.30
• *MAVFlow (ours)*				
C5	GT AV Speech Unit	**8.30**	6.81	5.69

Subjective evaluation. To evaluate the naturalness of the generated speech, we assessed the MOS scores for the translated speech from the MuAViC dataset generated by each system in Table 4. The evaluation results show that our naturalness quality achieved higher MOS scores (3.49 for Similarity, 4.01 for Naturalness) compared to other cascade systems and AV2AV (3.33 for Similarity, 3.58 for Naturalness).

5.5. Zero-shot Video Translation Result

Visual generation quality. In Table 5, we evaluated the visual quality of the generated videos and the synchronization between the audio and visual components. MAVFlow achieves an LSE-C score of 8.30, outperforming all baseline methods. Particularly, when compared to AV2AV (C4), which has a similar direct synchronization structure to ours, MAVFlow demonstrates significant improvements across all metrics: LSE-C (+0.87), LSE-D (−0.49), and FID (−0.61). These results indicate that audio-visual guidance not only enhances the consistency of synthesized speech but also positively affects face generation quality.

Specifically, the high LSE-C score highlights a strong correlation between the generated audio and video, suggesting that MAVFlow effectively utilized visual embeddings. In other words, our model successfully integrated latent visual information from the initial stages of mel-spectrogram generation through visual guidance. Additionally, the synthesized face images, based on high-quality mel-spectrograms, also exhibited competitive performance in the FID metric, confirming the generation of more natural and realistic faces.

Visual emotional quality. In Figure 3, we analyze the generated visual quality on the CREMA-D dataset and evaluate whether each generated visual frame accurately reflects the speaker's emotion using a visual emotion recognition model. Through this evaluation, we confirm that our proposed method, which applies visual embedding at the frame level, effectively captures the original emotional state of the speaker over time. For instance, in Figure 3, the AV2AV method incorrectly predicted 'HAP' (Happy) for an original video labeled with 'ANG' (Anger). Upon examining

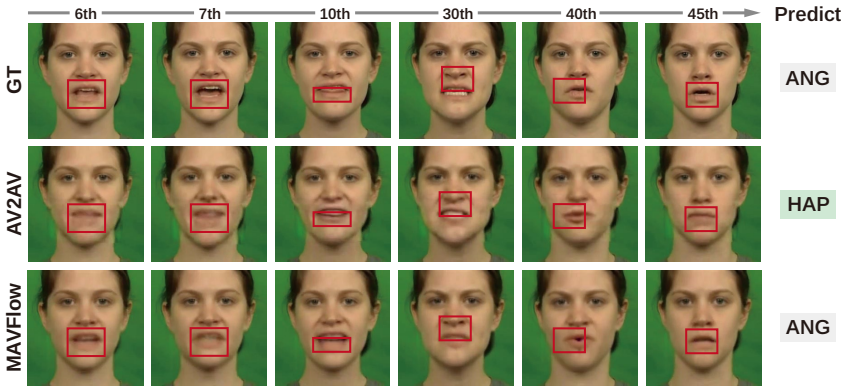

Figure 3. Visual analysis of emotional representation in generated videos. By applying speaker facial emotion embeddings at each frame, our approach enhances frame-level emotional accuracy. As highlighted by the rectangular boxes, our method effectively resolves emotion misclassification issues found in the AV2AV.

Table 6. Visual emotion recognition accuracy (Emo-Acc) and emotion embedding cosine similarity (ES) measured from the generated visual results on CREMA-D.

Method	Emo-Acc (%) ↑	ES ↑
GT	76.83	1.00
AV2AV	67.20	0.87
MAVFlow (ours)	**72.68**	**0.92**

Table 7. Audio emotion accuracy and embedding cosine similarity (ES) after additional training (+: additional training on CREMA-D).

Method	Emo-Acc (%) ↑	ES ↑	SS ↑
AV2AV	33.66	0.84	0.33
MAVFlow	36.46	0.86	0.39
MAVFlow +	**51.46**	**0.90**	**0.49**

each frame closely, it becomes clear that the video generated by AV2AV fails to adequately express the anger emotion, particularly around the mouth, compared to the ground truth video. These visual observations are further supported by the quantitative results in Table 6, which show that while AV2AV's visual emotion recognition performance decreases compared to the ground truth, our proposed method demonstrates better preservation not only in terms of accuracy (Emo-Acc) but also in embedding similarity (ES). Additional visual quality can be referred to in Appendix A.

5.6. Ablation Study

Additional training on emotion dataset. In Table 2, we only trained our model on the MuAViC dataset to enable zero-shot evaluation on the unseen CREMA-D benchmark. However, additional training on emotion-rich audio-visual datasets can significantly enhance emotion transfer performance. In Table 7, we lightly uptrained MAVFlow on CREMA-D training datasets (referred to as MAVFlow+), resulting in a notable increase in Emo-Acc from 36.46% to 51.46% as well as an improvement in ES from 0.86 to 0.90. Since MAVFlow outperformed the baselines using only MuAViC, we expect that incorporating such emotion-rich data would further widen this performance gap.

Effect of audio-visual guidance. We conducted an ablation study to examine the effect of each modality guidance on audio generation. Table 8 presents the results of evaluating the effect of audio and visual modality guidance on emotion recognition using the CREMA-D audio dataset. Additionally, it includes the analysis of results from translating audio in Es, Fr, It, and Pt to En using the MuAViC dataset, based on the settings outlined in Table 1. The SS and MCD-DTW values in Table 8 were averaged across each language for analysis. As a result, we observed

Table 8. Ablation study for the effect of modality guidance on CREMA-D and MuAViC translation.

		CREMA-D		MuAViC	
Audio	**Visual**	**SS ↑**	**Emo-Acc ↑**	**SS ↑**	**DTW ↓**
✗	✗	0.167	28.66	0.057	10.13
✗	✓	0.174	26.83	0.056	10.73
✓	✗	**0.391**	35.85	0.487	7.50
✓	✓	0.388	**36.46**	**0.504**	**7.37**

that when both audio and visual guidance were provided, speaker similarity and emotional accuracy improved. One interesting observation is that when visual guidance is provided alone, speaker similarity slightly increases or is maintained (as seen in Table 8), but Emo-Acc decreases. This suggests that visual guidance alone has a minimal effect on maintaining emotion, and its complementary effect is maximized when combined with audio guidance.

6. Conclusion

In this paper, we introduced MAVFlow, a zero-shot audio-visual translation framework utilizing Conditional Flow Matching (CFM) to address speaker consistency challenges inherent in existing AV2AV methods. By effectively integrating paralinguistic characteristics from both audio and visual modalities, MAVFlow significantly enhances speaker consistency across languages without intermediate text representations. Our method leverages discrete speech units and dual-modal guidance to synthesize high-quality mel-spectrograms, resulting in improved lip synchronization, emotional accuracy, and overall visual quality. Experimental evaluations on the MuAViC and CREMA-D datasets confirm that MAVFlow outperforms prior AV2AV methods, establishing it as a robust and efficient solution for multilingual audio-visual translation.

Acknowledgements

This work was supported by Institute of Information & communications Technology Planning & Evaluation (IITP) grant funded by the Korea government (MSIT) [No. 2022-0-00641, XVoice: Multi-Modal Voice Meta Learning], [No. RS-2024-00457882, AI Research Hub Project], and [No. 2019-0-00075, Artificial Intelligence Graduate School Program (KAIST)].

References

[1] Prottay Kumar Adhikary, Bandaru Sugandhi, Subhojit Ghimire, Santanu Pal, and Partha Pakray. Travid: An end-to-end video translation framework. *arXiv preprint arXiv:2309.11338*, 2023. 2

[2] Triantafyllos Afouras, Joon Son Chung, and Andrew Zisserman. Lrs3-ted: a large-scale dataset for visual speech recognition. *arXiv preprint arXiv:1809.00496*, 2018. 5

[3] Mohamed Anwar, Bowen Shi, Vedanuj Goswami, Wei-Ning Hsu, Juan Pino, and Changhan Wang. Muavic: A multilingual audio-visual corpus for robust speech recognition and robust speech-to-text translation. *arXiv preprint arXiv:2303.00628*, 2023. 1, 2, 5, 6

[4] Andreas Blattmann, Tim Dockhorn, Sumith Kulal, Daniel Mendelevitch, Maciej Kilian, Dominik Lorenz, Yam Levi, Zion English, Vikram Voleti, Adam Letts, et al. Stable video diffusion: Scaling latent video diffusion models to large datasets. *arXiv preprint arXiv:2311.15127*, 2023. 2

[5] William Brannon, Yogesh Virkar, and Brian Thompson. Dubbing in practice: A large scale study of human localization with insights for automatic dubbing. *Transactions of the Association for Computational Linguistics*, 11:419–435, 2023. 2

[6] Houwei Cao, David G Cooper, Michael K Keutmann, Ruben C Gur, Ani Nenkova, and Ragini Verma. Crema-d: Crowd-sourced emotional multimodal actors dataset. *IEEE transactions on affective computing*, 5(4):377–390, 2014. 2, 5

[7] Edresson Casanova, Julian Weber, Christopher D Shulby, Arnaldo Candido Junior, Eren Gölge, and Moacir A Ponti. Yourtts: Towards zero-shot multi-speaker tts and zero-shot voice conversion for everyone. In *International conference on machine learning*, pages 2709–2720. PMLR, 2022. 1, 5, 6, 7

[8] Edresson Casanova, Kelly Davis, Eren Gölge, Görkem Göknar, Iulian Gulea, Logan Hart, Aya Aljafari, Joshua Meyer, Reuben Morais, Samuel Olayemi, et al. Xtts: a massively multilingual zero-shot text-to-speech model. *arXiv preprint arXiv:2406.04904*, 2024. 1, 5, 6, 7

[9] Qi Chen, Mingkui Tan, Yuankai Qi, Jiaqiu Zhou, Yuanqing Li, and Qi Wu. V2c: Visual voice cloning. In *Proceedings of the IEEE/CVF Conference on Computer Vision and Pattern Recognition*, pages 21242–21251, 2022. 6

[10] Ting Chen, Marco Tagliasacchi, Ron J. Weiss, Kanishka Rao, Peter Rowe, and Mohammad Norouzi. WaveGrad 2: Iterative refinement for text-to-speech synthesis. In *Proceedings of the 22nd Annual Conference of the International Speech Communication Association (Interspeech)*, pages 4832–4836, 2021. 2

[11] Yafeng Chen, Siqi Zheng, Hui Wang, Luyao Cheng, Qian Chen, and Jiajun Qi. An enhanced res2net with local and global feature fusion for speaker verification. *arXiv preprint arXiv:2305.12838*, 2023. 5

[12] Xize Cheng, Rongjie Huang, Linjun Li, Tao Jin, Zehan Wang, Aoxiong Yin, Minglei Li, Xinyu Duan, Zhou Zhao, et al. Transface: Unit-based audio-visual speech synthesizer for talking head translation. *arXiv preprint arXiv:2312.15197*, 2023. 1, 2, 3, 5

[13] Jeongsoo Choi, Se Jin Park, Minsu Kim, and Yong Man Ro. Av2av: Direct audio-visual speech to audio-visual speech translation with unified audio-visual speech representation. In *Proceedings of the IEEE/CVF Conference on Computer Vision and Pattern Recognition*, pages 27325–27337, 2024. 1, 2, 3, 4, 5, 12

[14] Joon Son Chung, Arsha Nagrani, and Andrew Zisserman. Voxceleb2: Deep speaker recognition. *arXiv preprint arXiv:1806.05622*, 2018. 5

[15] Marta R Costa-Jussà, James Cross, Onur Çelebi, Maha Elbayad, Kenneth Heafield, Kevin Heffernan, Elahe Kalbassi, Janice Lam, Daniel Licht, Jean Maillard, et al. No language left behind: Scaling human-centered machine translation. *arXiv preprint arXiv:2207.04672*, 2022. 1

[16] Prafulla Dhariwal and Alexander Quinn Nichol. Diffusion models beat GANs on image synthesis. In *Advances in Neural Information Processing Systems (NeurIPS)*, pages 8780–8794, 2021. 2

[17] Zhihao Du, Qian Chen, Shiliang Zhang, Kai Hu, Heng Lu, Yexin Yang, Hangrui Hu, Siqi Zheng, Yue Gu, Ziyang Ma, et al. Cosyvoice: A scalable multilingual zero-shot text-to-speech synthesizer based on supervised semantic tokens. *arXiv preprint arXiv:2407.05407*, 2024. 3

[18] Patrick Esser, Sumith Kulal, Andreas Blattmann, Rahim Entezari, Jonas Müller, Harry Saini, Yam Levi, Dominik Lorenz, Axel Sauer, Frederic Boesel, et al. Scaling rectified flow transformers for high-resolution image synthesis. In *Forty-first international conference on machine learning*, 2024. 2

[19] Angela Fan, Shruti Bhosale, Holger Schwenk, Zhiyi Ma, Ahmed El-Kishky, Siddharth Goyal, Mandeep Baines, Onur Celebi, Guillaume Wenzek, Vishrav Chaudhary, et al. Beyond english-centric multilingual machine translation. *Journal of Machine Learning Research*, 22(107):1–48, 2021. 1, 6

[20] Marcello Federico, Robert Enyedi, Roberto Barra-Chicote, Ritwik Giri, Umut Isik, Arvindh Krishnaswamy, and Hassan Sawaf. From speech-to-speech translation to automatic dubbing. In *Proceedings of the 17th International Conference on Spoken Language Translation*, pages 257–264, 2020. 1

[21] Peng Gao, Le Zhuo, Dongyang Liu, Ruoyi Du, Xu Luo, Longtian Qiu, Yuhang Zhang, Chen Lin, Rongjie Huang, Shijie Geng, et al. Lumina-t2x: Transforming text into any modality, resolution, and duration via flow-based large diffusion transformers. *arXiv preprint arXiv:2405.05945*, 2024. 3

[22] Martin Heusel, Hubert Ramsauer, Thomas Unterthiner, Bernhard Nessler, and Sepp Hochreiter. Gans trained by a two time-scale update rule converge to a local nash equilibrium. *Advances in neural information processing systems*, 30, 2017. 6

[23] Jonathan Ho, Ajay Jain, and Pieter Abbeel. Denoising diffusion probabilistic models. In *Advances in Neural Information Processing Systems (NeurIPS)*, pages 6840–6851, 2020. 2

[24] Jonathan Ho, Tim Salimans, Alexey Gritsenko, William Chan, Mohammad Norouzi, and David J Fleet. Video diffusion models. *Advances in Neural Information Processing Systems*, 35:8633–8646, 2022. 2

[25] Rongjie Huang, Huadai Liu, Xize Cheng, Yi Ren, Linjun Li, Zhenhui Ye, Jinzheng He, Lichao Zhang, Jinglin Liu, Xiang Yin, et al. Av-transpeech: Audio-visual robust speech-to-speech translation. In *Proceedings of the 61st Annual Meeting of the Association for Computational Linguistics (Volume 1: Long Papers)*, pages 8590–8604, 2023. 1

[26] Myeonghun Jeong, Hyeongju Kim, Sung Jun Cheon, Byoung Jin Choi, and Nam Soo Kim. Diff-tts: A denoising diffusion model for text-to-speech. *arXiv preprint arXiv:2104.01409*, 2021. 2

[27] Ye Jia, Ron J. Weiss, Yuan Cao, Jinsung Choi, et al. Direct speech-to-speech translation with a sequence-to-sequence model. In *Proceedings of the 20th Annual Conference of the International Speech Communication Association (Interspeech)*, pages 1123–1127, 2019. 2

[28] Ye Jia, Michelle Tadmor Ramanovich, Tal Remez, and Roi Pomerantz. Translatotron 2: High-quality direct speech-to-speech translation with voice preservation. In *International Conference on Machine Learning*, pages 10120–10134. PMLR, 2022. 2

[29] Minsu Kim, Jeongsoo Choi, Dahun Kim, and Yong Man Ro. Textless unit-to-unit training for many-to-many multilingual speech-to-speech translation. *IEEE/ACM Transactions on Audio, Speech, and Language Processing*, 2024. 2, 6

[30] Jungil Kong, Jaehyeon Kim, and Jaekyoung Bae. Hifi-gan: Generative adversarial networks for efficient and high fidelity speech synthesis. *Advances in neural information processing systems*, 33:17022–17033, 2020. 2, 5

[31] Zhifeng Kong, Wei Ping, Jiaji Huang, Kexin Zhao, and Bryan Catanzaro. DiffWave: A versatile diffusion model for audio synthesis. In *International Conference on Learning Representations (ICLR)*, 2021. 2

[32] Cees M Koolstra, Allerd L Peeters, and Herman Spinhof. The pros and cons of dubbing and subtitling. *European journal of communication*, 17(3):325–354, 2002. 1, 2

[33] Prajwal KR, Rudrabha Mukhopadhyay, Jerin Philip, Abhishek Jha, Vinay Namboodiri, and CV Jawahar. Towards automatic face-to-face translation. In *Proceedings of the 27th ACM international conference on multimedia*, pages 1428–1436, 2019. 2

[34] Matthew Le, Apoorv Vyas, Bowen Shi, Brian Karrer, Leda Sari, Rashel Moritz, Mary Williamson, Vimal Manohar, Yossi Adi, Jay Mahadeokar, et al. Voicebox: Text-guided multilingual universal speech generation at scale. *Advances in neural information processing systems*, 36:14005–14034, 2023. 2

[35] Ann Lee, Hongyu Gong, Paul-Ambroise Duquenne, Holger Schwenk, Peng-Jen Chen, Changhan Wang, Sravya Popuri, Yossi Adi, Juan Pino, Jiatao Gu, et al. Textless speech-to-speech translation on real data. *arXiv preprint arXiv:2112.08352*, 2021. 2

[36] Yaron Lipman, Ricky TQ Chen, Heli Ben-Hamu, Maximilian Nickel, and Matt Le. Flow matching for generative modeling. *arXiv preprint arXiv:2210.02747*, 2022. 2, 3

[37] Xingchao Liu, Chengyue Gong, and Qiang Liu. Flow straight and fast: Learning to generate and transfer data with rectified flow. *arXiv preprint arXiv:2209.03003*, 2022. 2

[38] Xingchao Liu, Xiwen Zhang, Jianzhu Ma, Jian Peng, et al. Instaflow: One step is enough for high-quality diffusion-based text-to-image generation. In *The Twelfth International Conference on Learning Representations*, 2023. 2

[39] Nanye Ma, Mark Goldstein, Michael S Albergo, Nicholas M Boffi, Eric Vanden-Eijnden, and Saining Xie. Sit: Exploring flow and diffusion-based generative models with scalable interpolant transformers. In *European Conference on Computer Vision*, pages 23–40. Springer, 2024. 2

[40] Ziyang Ma, Zhisheng Zheng, Jiaxin Ye, Jinchao Li, Zhifu Gao, Shiliang Zhang, and Xie Chen. emotion2vec: Self-supervised pre-training for speech emotion representation. *arXiv preprint arXiv:2312.15185*, 2023. 6, 7, 12

[41] Evgeny Matusov, Nicola Ueffing, and Hermann Ney. Integration of speech recognition and machine translation in computer-assisted translation. In *Proceedings of the 9th International Conference on Spoken Language Processing (Interspeech/ICSLP)*, pages 641–644, 2006. 2

[42] Evgeny Matusov, Patrick Wilken, and Yota Georgakopoulou. Customizing neural machine translation for subtitling. In *Proceedings of the Fourth Conference on Machine Translation (Volume 1: Research Papers)*, pages 82–93, 2019. 1

[43] Harry McGurk and John MacDonald. Hearing lips and seeing voices. *Nature*, 264(5588):746–748, 1976. 1, 2

[44] Shivam Mehta, Ruibo Tu, Jonas Beskow, Éva Székely, and Gustav Eje Henter. Matcha-tts: A fast tts architecture with conditional flow matching. In *ICASSP 2024-2024 IEEE International Conference on Acoustics, Speech and Signal Processing (ICASSP)*, pages 11341–11345. IEEE, 2024. 2, 3

[45] Chong Mou, Xintao Wang, Liangbin Xie, Yanze Wu, Jian Zhang, Zhongang Qi, and Ying Shan. T2i-adapter: Learning adapters to dig out more controllable ability for text-to-image diffusion models. In *Proceedings of the AAAI conference on artificial intelligence*, pages 4296–4304, 2024. 3

[46] Eliya Nachmani, Alon Levkovitch, Yifan Ding, Chulayuth Asawaroengchai, Heiga Zen, and Michelle Tadmor Ramanovich. Translatotron 3: Speech to speech translation with monolingual data. In *ICASSP 2024-2024 IEEE International Conference on Acoustics, Speech and Signal Processing (ICASSP)*, pages 10686–10690. IEEE, 2024. 2

[47] Hermann Ney, Frank Wessel, and Klaus Macherey. Speech translation: Coupling recognition and translation. In *Proceedings of the IEEE International Conference on Acoustics, Speech, and Signal Processing (ICASSP)*, pages 517–520, 1999. 2

[48] Kishore Papineni, Salim Roukos, Todd Ward, and Wei-Jing Zhu. Bleu: a method for automatic evaluation of machine translation. In *Proceedings of the 40th annual meeting of the Association for Computational Linguistics*, pages 311–318, 2002. 6

[49] Se Jin Park, Minsu Kim, Joanna Hong, Jeongsoo Choi, and Yong Man Ro. Synctalkface: Talking face generation with precise lip-syncing via audio-lip memory. In *Proceedings of the AAAI Conference on Artificial Intelligence*, pages 2062–2070, 2022. 1

[50] Vadim Popov, Alexey Vovk, Andrey Gogoryan, Mikhail Kudinov, Aaron van den Oord, Giulia Carmantini, and Anton Gusev. Grad-TTS: A diffusion probabilistic model for text-to-speech. In *International Conference on Machine Learning (ICML)*, pages 8599–8608, 2021. 2

[51] KR Prajwal, Rudrabha Mukhopadhyay, Vinay P Namboodiri, and CV Jawahar. A lip sync expert is all you need for speech to lip generation in the wild. In *Proceedings of the 28th ACM international conference on multimedia*, pages 484–492, 2020. 1, 2, 5, 6

[52] Alec Radford, Jong Wook Kim, Tao Xu, Greg Brockman, Christine McLeavey, and Ilya Sutskever. Robust speech recognition via large-scale weak supervision. In *International conference on machine learning*, pages 28492–28518. PMLR, 2023. 1

[53] Robin Rombach, Andreas Blattmann, Dominik Lorenz, Patrick Esser, and Björn Ommer. High-resolution image synthesis with latent diffusion models. In *Proceedings of the IEEE/CVF conference on computer vision and pattern recognition*, pages 10684–10695, 2022. 2

[54] Elizabeth Salesky, Matthew Wiesner, Jacob Bremerman, Roldano Cattoni, Matteo Negri, Marco Turchi, Douglas W Oard, and Matt Post. The multilingual tedx corpus for speech recognition and translation. *arXiv preprint arXiv:2102.01757*, 2021. 5

[55] Bowen Shi, Wei-Ning Hsu, Kushal Lakhotia, and Abdelrahman Mohamed. Learning audio-visual speech representation by masked multimodal cluster prediction. *International Conference on Learning Representations*, 2022. 2

[56] David Snyder, Daniel Garcia-Romero, Gregory Sell, Daniel Povey, and Sanjeev Khudanpur. X-vectors: Robust dnn embeddings for speaker recognition. In *2018 IEEE international conference on acoustics, speech and signal processing (ICASSP)*, pages 5329–5333. IEEE, 2018. 2, 4

[57] Joon Son Chung, Andrew Senior, Oriol Vinyals, and Andrew Zisserman. Lip reading sentences in the wild. In *Proceedings of the IEEE conference on computer vision and pattern recognition*, pages 6447–6456, 2017. 5

[58] Jiaming Song, Chenlin Meng, and Stefano Ermon. Denoising diffusion implicit models. *arXiv preprint arXiv:2010.02502*, 2020. 2

[59] Licai Sun, Zheng Lian, Bin Liu, and Jianhua Tao. Maedfer: Efficient masked autoencoder for self-supervised dynamic facial expression recognition. In *Proceedings of the 31st ACM International Conference on Multimedia*, pages 6110–6121, 2023. 6, 12

[60] Antoine Toisoul, Jean Kossaifi, Adrian Bulat, Georgios Tzimiropoulos, and Maja Pantic. Estimation of continuous valence and arousal levels from faces in naturalistic conditions. *Nature Machine Intelligence*, 3(1):42–50, 2021. 2, 4

[61] Alexander Tong, Kilian Fatras, Nikolay Malkin, Guillaume Huguet, Yanlei Zhang, Jarrid Rector-Brooks, Guy Wolf, and Yoshua Bengio. Improving and generalizing flow-based generative models with minibatch optimal transport. *arXiv preprint arXiv:2302.00482*, 2023. 3

[62] Ehsan Variani, Xin Lei, Erik McDermott, Ignacio Lopez Moreno, and Javier Gonzalez-Dominguez. Deep neural networks for small footprint text-dependent speaker verification. In *2014 IEEE international conference on acoustics, speech and signal processing (ICASSP)*, pages 4052–4056. IEEE, 2014. 2

[63] Apoorv Vyas, Bowen Shi, Matthew Le, Andros Tjandra, Yi-Chiao Wu, Baishan Guo, Jiemin Zhang, Xinyue Zhang, Robert Adkins, William Ngan, et al. Audiobox: Unified audio generation with natural language prompts. *arXiv preprint arXiv:2312.15821*, 2023. 3

[64] Alexander Waibel, Moritz Behr, Dogucan Yaman, Fevziye Irem Eyiokur, Tuan-Nam Nguyen, Carlos Mullov, Mehmet Arif Demirtas, Alperen Kantarci, Stefan Constantin, and Hazim Kemal Ekenel. Face-dubbing++: Lip-synchronous, voice preserving translation of videos. In *2023 IEEE International Conference on Acoustics, Speech, and Signal Processing Workshops (ICASSPW)*, pages 1–5. IEEE, 2023. 2

[65] Chengyi Wang, Sanyuan Chen, Yu Wu, Ziqiang Zhang, Long Zhou, Shujie Liu, Zhuo Chen, Yanqing Liu, Huaming Wang, Jinyu Li, et al. Neural codec language models are zero-shot text to speech synthesizers. *arXiv preprint arXiv:2301.02111*, 2023. 1

[66] Ron J. Weiss, Jan K. Chorowski, Navdeep Jaitly, Yonghui Wu, and Zhifeng Chen. Sequence-to-sequence models can directly translate foreign speech. *arXiv preprint arXiv:1703.08581*, 2017. 2

[67] Yi Yang, Brendan Shillingford, Yannis Assael, Miaosen Wang, Wendi Liu, Yutian Chen, Yu Zhang, Eren Sezener, Luis C Cobo, Misha Denil, et al. Large-scale multilingual audio visual dubbing. *arXiv preprint arXiv:2011.03530*, 2020. 2

[68] Heiga Zen, Viet Dang, Rob Clark, Yu Zhang, Ron J Weiss, Ye Jia, Zhifeng Chen, and Yonghui Wu. Libritts: A corpus derived from librispeech for text-to-speech. *arXiv preprint arXiv:1904.02882*, 2019. 5

[69] Hang Zhou, Yu Liu, Ziwei Liu, Ping Luo, and Xiaogang Wang. Talking face generation by adversarially disentangled audio-visual representation. In *Proceedings of the AAAI conference on artificial intelligence*, pages 9299–9306, 2019. 1

APPENDIX

A. Qualitative Results and Analysis

In Figure 4, we present dynamic emotional changes across frames within a single video at the first three frames from neutral to disgust. While MAVFlow effectively captures the emotional change of Ground Truth (GT) video from 15th frame, reflecting the shift starting from the 14th frame. AV2AV fails to reflect the emotion until around the 36th frame. Additionally, overall, MAVFlow better expresses emotions as well as the arousal level, which is indicated by the distance of a red dot from the center. Cascaded systems have been excluded from the comparison due to poor temporal alignment and their inability to embed emotional cues into the audio, which results in TFG output cannot reflect emotional expressions in the video. The DTW and DTW-SL metrics in Table 1 and Table 2, further confirm the notably poor temporal alignment of the cascaded systems.

B. Class-Wise Emotional Analysis

B.1. Audio Emotional Results

In Table 9, we evaluate the class-wise emotion recognition accuracy of the generated audio using the pretrained emotion2vec [40]. Compared to AV2AV, MAVFlow shows slightly lower performance for the Sad, Disgust, and Fear classes, while demonstrating comparable or superior results for Happy, Neutral, and Angry. Notably, MAVFlow exhibits a significant advantage in the Angry class, ultimately achieving better overall performance than AV2AV in both Emo-Acc and ES metrics (as shown in Table 7). Furthermore, the MAVFlow + model, trained with additional emotional datasets, achieves improved performance across most emotion classes, with a substantial gain in overall Emo-Acc.

Table 9. Class-wise emotion accuracy (%) of generated audio (+: additional training on CREMA-D).

Method	Happy	Sad	Neutral	Angry	Disgust	Fear	Emo-Acc ↑
GT	89.29	85.00	89.17	89.29	77.86	62.14	81.95
AV2AV	30.00	**22.86**	**80.00**	28.57	30.71	16.43	33.66
MAVFlow	36.43	11.43	**80.00**	62.86	20.00	14.29	36.46
MAVFlow +	**69.29**	**22.86**	66.67	**80.71**	**32.86**	**38.57**	**51.46**

B.2. Visual Emotional Results

In Table 10, we evaluated class-wise visual emotion accuracy using pretrained MAE-DFER [59]. Also, follow MAE-DFER, we report both Unweighted Average Recall (UAR) and Weighted Average Recall (WAR) as evaluation metrics. UAR calculates the average recall by treating each class equally, which helps account for class imbalance, while WAR weights the recall by the number of samples per class, reflecting the actual class distribution in the dataset. As a result, MAVFlow achieved strong performance in terms of both UAR and WAR, particularly excelling in the angry, disgust, and fear emotion classes.

C. Inference Time Comparison

MAVFlow does not rely on intermediate text representations, resulting in faster inference compared to the cascaded system. Furthermore, it is more efficient by applying the speed-friendly CFM module compare to diffusion model. We compared the inference speed using one A6000 GPU, observing processing times of 1.66s for MAVFlow, 1.22s for AV2AV, and 1.75s for the 4-cascaded model to handle a 2.35s audio-visual input through the complete pipeline.

D. Limitation

MAVFlow currently leverages emotional embeddings only from face and speaker embeddings from audio. However, we believe that incorporating emotional cues from audio (*e.g.*, prosody, timbre, and other paralinguistic features) into the guidance of CFM could further enhance performance. Furthermore, since we directly adopt the unit extractor and unit-to-unit translation modules from previous work [13], improving semantic translation quality remains an open challenge.

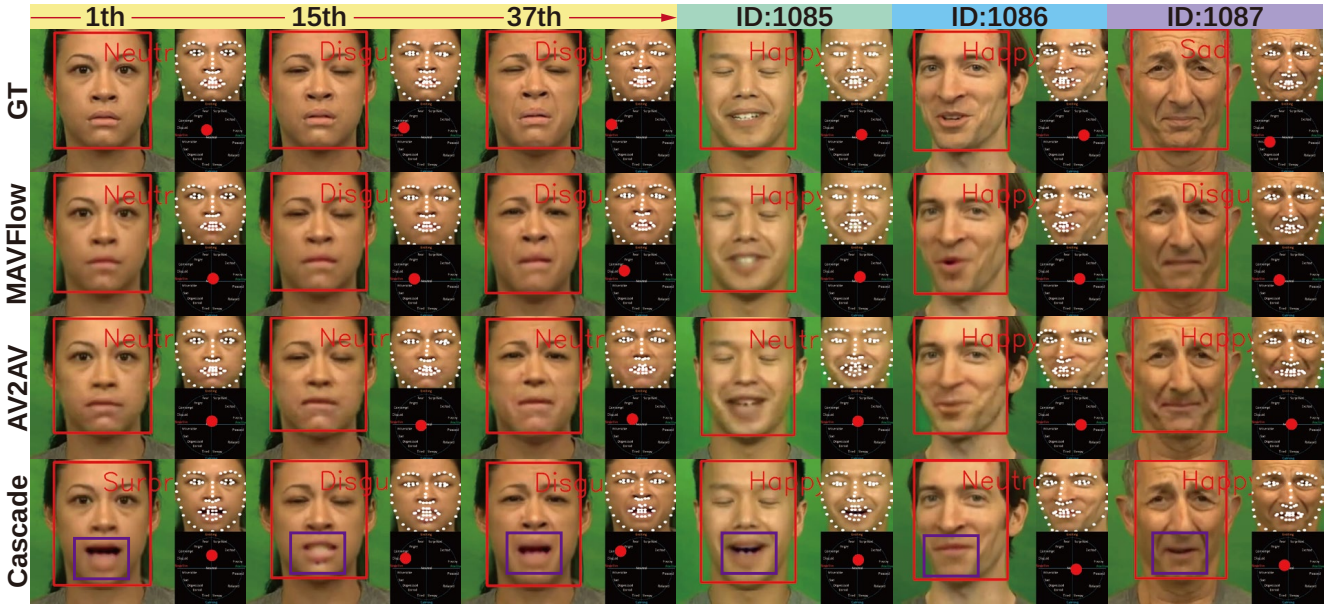

Figure 4. Additional qualitative comparison for frame-level analysis. Each row shows GT, MAVFlow, AV2AV, and Cascade (ASR+XTTS+TFG), respectively.

Table 10. Class-wise emotion accuracy, unweighted and weighted average recall (UAR%, WAR%), and ES of the generated visuals, all measured with MAE-DFER (+: additional training on CREMA-D).

Method	Happy	Sad	Neutral	Angry	Disgust	Fear	UAR	WAR	ES
GT	97.14	67.86	76.67	78.57	87.86	52.86	76.83	76.83	1.00
ASR+YourTTS+TFG	89.86	60.71	72.88	50.71	83.57	40.00	66.29	66.05	0.85
ASR+XTTS+TFG	94.93	55.00	72.03	72.86	85.71	31.43	68.66	68.50	0.91
AV2AV	**95.00**	**64.29**	**79.17**	62.14	77.14	27.14	67.48	67.20	0.87
MAVFlow	**95.00**	53.57	75.00	**80.71**	**88.57**	**43.57**	72.74	72.68	0.92
MAVFlow +	**95.00**	63.57	78.33	76.43	87.14	37.86	**73.06**	**72.93**	**0.93**